

**ELECTROMAGNETIC SHIELDING EFFECTIVENESS OF CEMENT POWDER
MIXED WITH GRAPHITE FOR MITIGATION AGAINST
ELECTROMAGNETIC INTERFERENCE**

YEE SEE KHEE

**A thesis submitted in
fulfillment of the requirement for the award of the
Doctor of Philosophy**

**Faculty of Electrical and Electronic Engineering
Universiti Tun Hussein Onn Malaysia**

March, 2015

ABSTRACT

The potentially harmful impacts of electromagnetic interference (EMI) on the safe operation of electronic and electrical equipment are drawing serious attention due to reliance on electrical and electronic devices in telecommunication, mobile phone networks, radar systems, banking, public defence, and others. EMI induces unwanted voltage and currents on the victim device, thus affecting the performance of the devices. Electromagnetic shielding which is commonly applied as the last resort in reducing the radiated emission from digital circuitries is switching its territory to building construction in an attempt to provide similar benefits to the sensitive and critical equipment inside the building. It is reported that concrete constructed with different weight fractions of material, moisture content (MC), and the effect of reinforcement bar will produce different shielding effectiveness (SE). The parameters that determine the SE of building materials include their dielectric constant, loss tangent and relative permeability. These parameters can be obtained based on dielectric measurement. Dielectric measurements need to be repeated when the composition of the building material changes. In this work, the SE of cement powder with additional additives, such as graphite powder, iron powder and nickel-zinc ferrite powder were investigated. It has been found that dielectric constant determines the trend of the reflection loss as it plays significant roles in establishing the characteristic impedance of the material. On the other hand, absorption loss and multiple reflection loss are more dependent on the thickness of material. Based on the results, it is recognised that graphite powder is an efficient and practical additive in enhancing the SE of cement powder compared with others. Cement-graphite powder provides more than 60 dB of shielding in between 200 MHz to 2000 MHz when the percentage of the graphite powder in the mixture is 30% and the thickness is 10 cm. Novel predictions, which are based on the neural network and piece-wise fitting has been proposed to predict the SE of cement-graphite mixture with different percentages of graphite powder. SE predictions which are based on piece-wise fitting and neural network produces 1.94 dB and 0.029 dB of error at 900 MHz and 1800 MHz respectively when it is used to predict the SE of cement-graphite that contains a 17% of graphite in between 100 MHz to 2000 MHz. In summary, this research investigates the effect of different additives on the SE of cement powder. The prediction based on the neural network indicates a sample with a thickness of 7 cm and 30% graphite is able to provide above 40 dB of shielding ranging between 100 MHz and 2000 MHz. Such prediction can be anticipated for implementation in building construction design.

ABSTRAK

Gangguan elektromagnet (EMI) telah menarik perhatian yang serius memandangkan terdapat pergantungan terhadap alatan elektrik dan elektronik di bidang telekomunikasi, rangkaian telefon mudah alih, sistem radar, perbankan, pertahanan awam dan lain-lain. EMI menghasilkan arus yang tidak diingini pada alatan mangsa tersebut dan seterusnya menjejaskan prestasi alatan itu. Perisai elektromagnet yang biasa digunakan dalam mengurangkan kesan radiasi daripada litar-litar digital mulai digunapakai dalam bidang pembinaan bangunan supaya ia boleh memberikan manfaat yang sama kepada alatan yang sensitif dan kritikal di dalam bangunan. Adalah dilaporkan bahawa konkrit yang dihasilkan dengan pelbagai pecahan berat bahan-bahan, kandungan lembapan (MC), dan kesan batang penetulang akan memberikan keberkesanan perisai (SE) yang berbeza. Parameter-parameter yang menentukan SE bagi bahan binaan termasuklah pemalar dielektrik, tangen kehilangan dan kebolehtelapan nisbi. Parameter-parameter tersebut boleh didapati daripada pengukuran dielektrik. Pengukuran dielektrik ini perlu diulangi apabila terdapat perubahan pada komposisi bahan binaan. Dalam penyelidikan ini, SE bagi serbuk simen yang dicampurkan dengan bahan tambahan seperti serbuk grafit, serbuk besi dan serbuk nikel-zink ferit telah dikaji. Adalah didapati bahawa, pemalar dielektrik menentukan trend bagi kehilangan pantulan kerana ia memainkan peranan yang penting dalam pengiraan galangan ciri sesuatu bahan. Sebaliknya, kehilangan penyerapan dan kehilangan pelbagai pantulan adalah lebih bergantung kepada ketebalan bahan itu. Berdasarkan kepada keputusan, didapati serbuk grafit merupakan bahan tambahan yang cekap dalam meningkatkan SE bagi serbuk simen sekiranya dibandingkan dengan serbuk tambahan yang lain. Serbuk simen-grafit memberikan SE yang melebihi 60 dB di antara 200 MHz to 2000 MHz apabila peratusan serbuk grafit ialah 30% dan ketebalan ialah 10 cm. Ramalan novel yang berdasarkan rangkaian neural dan kelengkapan secebis telah dicadangkan untuk meramalkan SE bagi campuran simen-grafit yang mengandungi pelbagai peratusan grafit. Ramalan SE yang berdasarkan kelengkapan secebis dan rangkaian neural telah menghasilkan ralat sebanyak 1.94 dB and 0.029 dB pada 900 MHz dan 1800 MHz masing-masing apabila digunakan untuk meramal SE bagi campuran simen-grafit yang mengandungi 17% grafit di antara 200 MHz to 2000 MHz. Ramalan yang berdasarkan rangkaian neural menunjukkan sampel yang mempunyai ketebalan 7 cm dan mengandungi 30% grafit berupaya untuk memberikan perisai lebih daripada 40 dB di antara 100 MHz and 2000 MHz. Ramalan ini dijangka bakal digunakan dalam reka bentuk pembinaan bangunan.

TABLE OF CONTENTS

DECLARATION	iii
DEDICATION	iv
ACKNOWLEDGEMENT	v
ABSTRACT	vi
ABSTRAK	vii
TABLE OF CONTENTS	viii
LIST OF TABLES	xi
LIST OF FIGURES	xiii
LIST OF SYMBOLS AND ABBREVIATIONS	xviii
LIST OF APPENDICES	xxi
LIST OF PUBLICATIONS	xxii
LIST OF AWARDS	xxiv
CHAPTER 1 INTRODUCTION	1
1.1 General	1
1.2 Problem Statement	3
1.3 Aim of the Research	5
1.4 Objectives of the Research	5
1.5 Limitations of the Research	5
1.6 Organization of the Thesis	6

CHAPTER 2 LITERATURE REVIEW	7
2.1 General	7
2.2 High Power Electromagnetic (HPEM)	8
2.3 Theory of Shielding Effectiveness	14
2.3.1 Near-field and Far-field Shielding	20
2.4 SE Determination	23
2.5 Shielding Effectiveness of Enhanced Building Material	31
2.6 Artificial Neural Network	36
2.7 Context of the Research	37
CHAPTER 3 METHODOLOGY	40
3.1 Samples Preparation	41
3.1.1 Preparation of Nickel-Zinc Ferrite Powder	43
3.2 Dielectric Measurement Devices	45
3.2.1 TEM Parallel Plates Measurement Method	45
3.2.2 APC-7 Connectors Measurement Method	53
3.3 Analytical Calculation of the Shielding Effectiveness (SE)	59
3.4 Verification of Analytical SE based on Computer Simulation	59
3.5 Shielding Effectiveness Predictions	61
3.5.1 Neural Network for SE Prediction	61
3.5.2 Piece-wise Fittings for SE Prediction	67
3.6 Experimental Measurement of SE	70
CHAPTER 4 RESULTS AND DISCUSSION	71
4.1 The Effectiveness of Parallel Plates and APC-7 Connectors for Dielectric Measurement	72
4.2 Dielectric Properties of Cement Powder with Additives	75
4.2.1 Cement Power Mixed with Graphite powder	75
4.2.2 Cement Power Mixed with Iron Powder	79
4.2.3 Cement Power Mixed with Nickel-Zinc Ferrite Powder	81
4.2.4 Uncertainty in Dielectric Measurement	87
4.3 Analytical Calculation of SE Based on Measured Dielectric Properties	92

4.3.1	Reflection loss, R_{dB}	92
4.3.2	Absorption Loss, A_{dB}	97
4.3.3	Multiple Reflection Loss, M_{dB}	101
4.3.4	Total Shielding Effectiveness	105
4.4	Sensitivity Analysis	109
4.4.1	Characteristic Impedance	110
4.4.2	Propagation Constant	111
4.4.3	Reflection Loss	112
4.4.4	Absorption Loss	113
4.4.5	Multiple Reflection Loss	113
4.5	Comparison of Analytical, Simulation and Experimental Results	116
4.6	Electromagnetic Prediction of Shielding Effectiveness Using Piece-wise Fitting and Neural Network	118
4.6.1	SE comparison for 1 cm Thick of Sample	119
4.6.2	SE comparison for 15 cm Thick of Sample	121
4.6.3	SE comparison for 10 cm Thick of Sample	124
4.7	Application of SE Prediction	130
4.8	Review of Achievements	134
4.9	Limitation of the Research	135
CHAPTER 5	CONCLUSION AND FUTURE RECOMMENDATIONS	137
5.1	Conclusion	137
5.2	Recommendation for Future Works	138
	REFERENCES	139
	APPENDIX A	148
	APPENDIX B	154
	APPENDIX C	157
	APPENDIX D	162

CHAPTER 1

INTRODUCTION

1.1 General

Exposure to electromagnetic (EM) fields is not a new phenomenon. Environmental exposure to man-made electromagnetic fields has been steadily increasing in line with growing of ever-advancing technologies. In order to fulfil the demand of the users in executing complicated tasks, the complexity of electronic devices has increased in the form of higher packing density and operating frequency. As a result, society has been exposed to a complex mix of weak electric and magnetic fields, both at home and in the workplace. This EM environment has created a new form of pollution known as electromagnetic pollution or electromagnetic interference (EMI), which consists of many unwanted radiated signals able to cause the unacceptable degradation of systems or equipment performance.

Common sources of EMI are from television and radio broadcasting-based stations, mobile phones and their stations, radar, power socket computers, high-voltage transmission lines and home-use electronic devices, such as microwave ovens, stereos receivers, irons, refrigerators, toasters, hair dryers, and so on. All of these devices unintentionally generate an EM field when they are operated. Table 1.1 lists the electric field strength and magnetic field strength of different home appliances at various distances, as published by World Health Organisation (WHO) (WHO, retrieved on 22 January 2014).

Table 1.1: Typical electric and magnetic field strengths measured near household appliances at various distance (WHO, retrieved on 22 January 2014).

Electrical Appliance	Electric field strength (V/m) at distance of 30cm	Magnetic field strength (μ T)		
		3cm	30cm	1m
Stereo receiver	180	No information		
Iron	120	8-30	0.12-0.3	0.01-0.03
Refrigerator	120	0.5-1.7	0.01-0.25	<0.01
Mixer	100	No information		
Toaster	80	No information		
Hair dryer	80	6-2000	0.01-7	0.01-0.03
Colour TV	60	2.5-50	0.04-2	0.01-0.15
Coffee machine	60	No information		
Vacuum cleaner	50	200-800	2-20	0.13-2
Electric oven	8	No information		
Light bulb	5	No information		
Electric shaver	No information	5-1500	0.08-9	0.01-0.03
Microwave oven	No information	73-200	4-8	0.25-0.6
Electric oven	No information	1-50	0.15-0.5	0.01-0.04

Besides the unintentional EMI, a new threat known as High-power electromagnetic (HPEM) has also emerged. HPEM generally describes a set of transient EM environments where the peak electric and magnetic fields can be intense. HPEM can be generated through lightning strikes, electrostatic discharge, specially designed microwave devices, and nuclear bursts. HPEM pulses are characterised by their fast rise time, broad frequency range, and high field strength. They introduce unwanted noise or signals into electric and electronic systems, thus disrupting, confusing or damaging these systems (Radasky, Baum, & Wik, 2004).

As society's dependence on information and automated mission-critical and safety-critical electronic systems is increasing, it is possible to envision the use of HPEM sources unintentionally causing upset or damage to a system. If these problems are left unattended, severe damage, or disruptions to the safety operations of other electronic devices may be seen. Therefore, there is a notable need for the effective shielding of electronic devices from adverse effects.

1.2 Problem Statement

The proliferation of electrical and electronic devices has driven society to live in an electromagnetic environment. According to WHO, tissue heating is the principal mechanism of interaction between radio frequency energy and the human body. At the frequencies used by mobile phones, most of the energy is absorbed by the skin and other superficial tissues, resulting in a negligible temperature rise in the brain and/or other organs of the body. However it is claimed by some of the researchers that exposure to the EM field causes health hazards, such as symptoms of languidness, insomnia, nervousness, headache, immunological malfunction and so on (Fesenko, Makar, Novoselova, & Sadovnikov, 1999; Jin Ouk Jang, 2002; Levitt & Lai, 2010). There are on-going researches centered on investigating the correlation between human health and EM exposure. This scenario indicates awareness of exposure to the EM field.

Moreover, the news releases by the United States (US) indicates that HPEM weapons represent one of the most likely and potentially devastating attack in the near future (Miller, 2005). HPEM is characterised by its fast rise time (notably less than a few thousandths of a second), broad frequency range (1 kHz–100 MHz) and high amplitude (between 5 kV/m and 50 kV/m), which is able to generate high voltage and current on every electrical conductor not designed to withstand this. It does not purely burn all the components on the printed circuit board (PCB), but rather melts them. The damage of the electronic and electrical system in banking, communication, automation and so on may prove to be a disaster for a nation.

Amongst all the hardenings suggested against EMI and HPEM, Faraday cage or shielding room is the most convenient when compared with hardening from the aspect of circuit design, which is not adequately tested. However the cost to build a shielding room which is made of metallic material is costly. Furthermore, it only

protects certain areas inside a building. So it is more meaningful and practical to embed the shielding capability directly within the building material as opposed to the building of faraday cages or shielding rooms inside the building. Such an approach not only protects the sensitive devices against the EMI, but also protects the human beings inside the building.

There are numerous researches being carried out concerned with investigating the way in which the shielding effectiveness (SE) of the building material can be improved (Cao & Chung, 2003, 2004; Guan, Liu, Duan, & Cheng, 2006; A. Ogunsola, Reggiani, & Sandrolini, 2009). Essentially, researches show that shielding materials and absorbing materials in the form of powder, fibre, or filament are efficient to be added into the building material to enhance the SE of the building material.

In order to analytically calculate the SE of a material, it is essential to establish the dielectric properties of the material. These parameters can be obtained by dielectric measurements. Most of the researches (Ellgardt & Mansson, 2013; A. Ogunsola, Reggiani, & Sandrolini, 2005; Soutsos, Bungey, Millard, Shaw, & Patterson, 2001) only report the dielectric properties of the building material when a certain percentage of additives are added into the building material and for every change of the material composition and percentage, dielectric measurement must be repeated. There is yet to be rigorous investigation performed on how the percentage of additives changes the dielectric properties of the building material in terms of formulation. Hence, it is necessary to have a prediction that is able to indicate the relationship between the percentages of the additive to the SE of the building material.

In this research, prediction tools able to estimate the SE of the cement powder added with different percentages of graphite powder is proposed. This provides the designer with guidelines on how to increase the SE of the cement powder with different percentages of graphite powder and thickness.

1.3 Aim of the Research

The aim of the research is to propose a prediction tool with the ability to calculate the SE of cement powder mixed with graphite where, based on this model, the designers can identify the SE of the cement powder with different thicknesses and percentages of graphite easily without carry out the dielectric measurement.

1.4 Objectives of the Research

1. To determine experimentally the relative permittivity and relative permeability of cement powder, cement-graphite powder, cement-iron powder and cement-nickel-zinc ferrite ($\text{Ni}_{0.5}\text{Zn}_{0.5}\text{Fe}_2\text{O}_4$) powder between 100 – 2000 MHz.
2. To determine the shielding effectiveness of cement-based material using measurements, analytical and prediction tools for different percentages of graphite powder.
3. To develop a neural network prediction tool with graphical user interface (GUI) which is able to calculate and display the SE of cement powder with various thicknesses and percentages of graphite powder.

1.5 Limitations of the Research

1. The SE of cement in powder form is investigated as it is a basic material in building construction. Concrete which is made of cement, sand, aggregates, stones and water may contributes to the SE uncertainties as too many parameters to be considered in the analysis, such as the moisture content of the concrete, size and impurities in the sand.
2. The incident electromagnetic wave is a linear, uniform plane wave, and normal incident on the surface of the cement powder.
3. The additives used in this research are graphite powder, iron powder and nickel-zinc ferrite ($\text{Ni}_{0.5}\text{Zn}_{0.5}\text{Fe}_2\text{O}_4$) powder.
4. Simple SE measurements using the APC-7 connectors are carried out.

5. Shielding effectiveness is analysed between 100 – 2000 MHz because it is occupied by applications such as television broadcasting, fixed wireless access, cellular mobile service, and so on. They are commonly exposed by the society.
6. The prediction techniques proposed in this research is based on neural network and piece-wise fitting.

1.6 Organization of the Thesis

The thesis comprises five individual chapters. Chapter 1 presents the background of the study, the problem statement, the objective of the study, and research limitations. Next in Chapter 2, it presents the latest, crucial literature reviews relating to this research, as well as some basic understanding about the concept of shielding. Chapter 3 describes the flow of the research, including the process of sample preparation, dielectric measurements, analytical formulation, simulation, experimental work and prediction. Chapter 4 highlights the results obtained following the completion of the experimental measurement, analytical formulation, simulation and prediction results. The findings based on the results are discussed. Finally chapter 5 concludes the research, and proposes future works for this research.

CHAPTER 2

LITERATURE REVIEWS

2.1 General

Research on Electromagnetic Fields (EMF) has been driven by public health considerations, as well as the overall perceived safety of electronic and electrical devices. There is a general public concern regarding the potential health effects associated with daily exposure for both children and adults. Adults, in particular, are of most concern due to their occupational exposure to EMF from mobile phone base stations, radio and television transmitters and occupational transmitters, such as, PVC welding machines, plasma etching, and military and civil radar systems operating at different frequencies (Bantsis, Sikalidis, Betsiou, Yioultsis, & Xenos, 2011).

Studies of human perception indicate that the greatest cutaneous sensitivity to microwave (MW) heating is at frequencies with wavelengths comparable to or smaller than the thickness of skin, the millimetre wave range (Bantsis et al., 2011). At frequencies spanning 1–10 GHz, much of the energy is absorbed below the superficial dermis (Barnes & Greenebaum, 2010). Some researchers have reported that EM waves can promote the growth of tumours in the human body (Beall, Delzell, Cole, & Brill, 1996; Grayson, 1996; Szmigielski, 1996).

Failures in electronic and electrical devices can be described as a disaster as human beings rely heavily on the electrical and electronic devices in the realm of banking, controlling systems, telecommunications, and so on. Therefore, materials for EMI protection have attracted considerable research attention for commercial and military applications. With EMI-shielding, electronic devices and confidential information is secure from device malfunctions due to EMI, with protection from

eavesdropping also achieved, as might arise from competitors or deterring electromagnetic forms of spying for military purposes, for example.

2.2 High Power Electromagnetic (HPEM)

A new threat which is known as high-power electromagnetic (HPEM) has emerged to civil society. It is a set of transient EM environments where peak electric and magnetic fields can be very high (Radasky et al., 2004). The typical environments considered as part of HPEM are the EM fields from nearby lightning strikes, the EM fields near an electrostatic discharge (ESD), the high-altitude electromagnetic pulse (HEMP) created by nuclear bursts, and high-power microwave (HPM) produced when a powerful chemical detonation is instantly transformed by a compression generator.

HEMP induces large voltage and current transients on electrical conductors, such as antennas, wires, as well as conductive tracks on electronic circuit boards. The efficiency of the energy transfer from the pulse to a system depends on frequency compatibility between the pulse and the entry path of the system and also the conductivity of the material. When the system characteristics match the offending HEMP pulse, higher levels of damage can occur (Miller, 2005). Overall, sophisticated integrated circuits with short signal paths are susceptible to high frequency pulses. Whilst large electrical systems, such as commercial power characterised by long transmission lines, are vulnerable to low frequency HEMP. HEMPs are typified by fast rise times, (volts/second), high field strengths (volts/meter (V/m), and broad frequency content (Hertz). The contributions of these factors will make them lethal to electronic systems.

Much attention has been directed towards the threat posed by HPEM against the function of important electronic systems of civil infrastructure, such as telecoms, radio/television, power networks or traffic control, financial systems, computer networks, and so on. In addition, the development of miniaturised pulsers and antenna systems has produced a situation where different types of intense EM field (narrowband to very wideband) can be produced at close ranges. With the development of more sophisticated computer equipment, along with the proximity of this equipment to the public, it is likely that criminals will use EM threat devices to

interfere with these computers, disrupting the ability of companies to provide important services to the public (IEEE P1642 D8, November 2011).

The damage produced by HEMP on electronic systems has occurred in the past. For instance, a military aircraft exposed to a ship's radar accidentally fired its munitions, which hit a fully fuelled aircraft on the deck. Besides this, when antilock braking systems (ABSs) were first introduced, problems arose in Germany on the autobahn, when brakes were applied when the autos passed a nearby radio transmitter. Not only that, the radio field emitted from the radio transmitter used in ambulance caused the attached monitor and defibrillator to shut down, causing the death of a 93-year-old heart attack patient (Leach & Alexander, 1995).

There are two major categories of EM environment of concern, namely narrowband and wideband, which can be delivered to a system through radiated and conducted technique. A narrowband waveform is almost a single frequency (typically a bandwidth of less than 1% of the centre frequency) of power delivered over a fixed time frame (from 100 nanoseconds to microseconds). For equipment vulnerabilities' testing due to radiated field, frequencies between 0.1 and 5 GHz seem to be of most concern. The narrowband threat usually requires very high power, and therefore high peak electric fields (usually greater than 100 V/m) (IEEE P1642 D8, November 2011) is produced. It is fairly easy to deliver fields on the order of thousands of V/m at a single frequency. Of course, each system under test may have a vulnerable frequency that is different from the next. Sometimes, the malfunctions observed in testing equipment with narrowband waveforms are those of permanent damage.

A wideband waveform (sometimes referred to as ultra wideband (UWB)) is usually one in which a time domain pulse is delivered, often in a repetitive fashion. The term 'wideband' indicates that the energy in the waveform is produced over a substantial frequency range relative to the 'centre frequency'. Four terms are used to describe the bandwidths of narrowband and wideband waveforms: hypoband, mesoband, sub-hyperband and hyperband. These terms have been defined based on the bandratio (ratio of high and low frequencies containing 90% of the energy), with values of <1.01, 1.01-3, 3-10, and >10, respectively (Giri & Tesche, 2004). Since a time domain pulse produces energy over many frequencies at the same time, the energy density at any single frequency is much less. This means that damage is not as likely as in the narrowband case. Importantly, however, it is easier to identify a

system's vulnerability since many frequencies are applied at the same time. Sources that have been built in the past typically produce repetitive pulses that can continue for many seconds or minutes, thereby increasing the probability of producing a system upset.

There are two primary ways by which EM pulse may be delivered to a computer equipment or system. One is through the application of radiated fields, whilst the other is through conduction along cables and wires. These two methods of delivery are consistent with the general treatment of EM disturbances in the field of electromagnetic compatibility (EMC). For radiated fields, frequencies above 100 MHz are of primary concern as they are able to penetrate unshielded or poorly protected buildings, and yet couple efficiently to the equipment inside of the building. In addition, they have the advantage that antennas designed to radiate efficiently at these frequencies are small. On the other hand, however, if conducted signals are injected into the power supply or telecom cables outside of a building, frequencies below 10 MHz (and pulse widths wider than 50 ns) propagate more efficiently than higher frequencies on cable shields and bundles (common mode) (IEEE P1642 D8, November 2011).

The level of susceptibility of electronic systems and the level of EM field that can be produced by an attacker is always a concern for the HPEM problem. The International Electrotechnical Commission (IEC) examined in IEC 61000-2-13 divides the EM weapons into three different types: low-tech (produced with magnetron from microwave oven, mid-tech IEMI source (commercial off-the-shelf radar system) and high-tech IEMI source (wideband pulsers) (IEC61000-2-13, 2005) Table 2.1 indicates the levels of narrowband fields that could be produced with different types of antennas (low-tech) for the 2.45 GHz signal (from magnetron of a microwave oven). The rE_{peak} represents an estimate of the strength of the EM field produced at a distance. One needs to divide the rE_{peak} (in volts) by the range in meters to obtain the peak field level in volts/meter as shown in Table 2.1.

Table 2.1: Levels of narrowband rE_{peak} and E_{peak} fields at three ranges using the magnetron of a microwave oven with different type of antennas (IEEE P1642 D8, November 2011).

Antenna type	Rms power (w)	Peak E-field in WR 340 kV/m	rE_{peak} V/m	E_{peak} V/m $r = 30$ m	E_{peak} V/m $r = 100$ m	E_{peak} V/m $r = 300$ m
Open-ended WR340	1100	25	540	18	5.4	1.8
Pyramidal Horn	1100	25	2200	73	22	7.3
Reflector antenna (1.8m diameter)	1100	25	4680	156	47	15.6

The narrowband field levels for two antennas, one large and the other more modest (mid-tech) are shown in Table 2.2. For the larger antenna, the rE_{peak} level is 1.9 MV, whilst for the smaller antenna, the rE_{peak} level is 0.6 MV. Dividing the rE_{peak} with the distance stated in Table 2.2, the values in the second and third column of the table can be obtained.

Table 2.2: Peak levels of narrowband electric fields at four ranges for 2 sizes of antennas produced by off-the-shelf radars considered to be mid-tech (IEEE P1642 D8, November 2011).

Range, r (m)	rE_{peak} , antenna size 9.35m ² kV/m	rE_{peak} , antenna size 0.935m ² kV/m
30	63	20
100	19	6
300	6.3	2
1000	1.9	0.6

Table 2.3 shows the wideband pulsed and impulse-radiating antennas that could be considered high-tech and built by national laboratories in several countries. The highest rE_{peak} level is 5 MV, as represented by the JOLT pulser.

Table 2.3: High-tech wideband pulser and IRAs circa 2003 (IEEE P1642 D8, November 2011)

Name	Pulser	Antenna (diameter)	Near field	Far field	rE_{peak} kV/m
Prototype IRA AFRL, KAFB, NM USA	± 60 kV 100ps/20ns 200 Hz burst	3.66 m	23 kV/m at $r=2$ m	4.2 kV/m at $r=304$ m	1280
Upgraded prototype IRA AFRL, KAFB, NM USA	± 75 kV 85ps/20ns ~ 400 Hz	1.83	41.6 kV/m at $r=16.6$ m	27.6 kV/m at $r=25$ m	690
Swiss IRA NEMP Laboratory Spiez, Switzerland	± 2.8 kV 100ps/4ns 800 Hz	1.8	1.4 kV/m at $r=5$ m	220 kV/m at $r=41$ m	10
TNO IRA The Hague Netherlands	± 9 kV 100ps/4ns 800 Hz	0.9	7 kV/m at $r=1$ m	Not available	34
University of Magdeburg, Magdeburg, Germany	± 9 kV 100ps/4ns 800 Hz	0.9	7 kV/m at $r=1$ m	Not available	34

Modern computers (with clock speeds of ~ 1 GHz), as well as other types of equipment using microprocessors, appear to be vulnerable from radiated narrowband fields above 200 V/m (depending on frequency). There appear to be large variations in the responses of equipment due to the specific experiment setups and the quality of the equipment enclosures used. In addition, tests performed on automobiles over the range of 1–15 GHz seem to indicate that malfunctions occur at lower field levels at lower frequencies. The malfunction of automobiles was reported by Bäckström at 500 V/m at 1.3 GHz for the testing performed in the mid-1990s (Bäckström, 1999). There are not many experimental results published to cover frequencies below 1 GHz. Tests performed on standalone PCs by Hoad indicates that this trend of lower level failures at lower frequencies continues down to 400 MHz (Richard Hoad, Carter, Herke, & Watkins, 2004). Other data indicate that, with the inclusion of network cables, susceptibility levels continue to decrease, with frequency of 100 MHz or possibly lower (R Hoad, Carter, Herke, Watkins, & Wraight, 2004).

Parfenov tested electronic cash registers to determine their susceptibility to hyperband waveforms with a 0.1/1 ns pulse (risetime/pulse width). Serious malfunctions occurred at peak values of ~ 2 kV/m and damage at ~ 5 kV/m (Radasky, 2006).

These experiments were performed by directly exposing the equipment under test within line of sight of a radiating antenna. If the equipment is inside a building or in a room without a window, there will be a reduction in the incident field. Besides this, the experiments do not thoroughly examine the polarisation and angle of incidence (except in mode-stirred chambers). Therefore, many of the serious effects noted during testing will actually occur at lower field levels when an optimum coupling geometry is applied, especially at frequencies above 1 GHz.

For conducted threats, if access to external telecom or power cables is not prevented, it is fairly easy to inject harmful signals into a building through power or communications cables. A comprehensive study performed by Parfenov indicates that both narrowband and wideband signals could be injected to the secondary of a building power supply, and these signals would propagate easily within the wiring of a building with limited attenuation. A related experimental study, performed by Parfenov, recognised that injected wideband pulsed voltages on the order of 5–6 kV could damage computer power supplies (Fortov et al., 2001). Experiments have also shown that narrowband voltages which are injected into the grounding system of a building can cause significant internal equipment malfunctions. Frequencies below 100 Hz and levels below 100 volts have been shown to cause problems.

For wideband-conducted transients, most of the lightning and electric fast transient tests for EMC immunity are performed for levels of up to 2 kV. Only in special cases, such as for equipment in a power-generating facility or a substation, the immunity test levels are higher. Typical EMC wideband test waveforms have rise-times as fast as 5 ns and pulse widths as long as 700 μ s. Moreover, many of the possible HPEM conducted threats have rise time greater than 1 ns and pulse widths on the order of a few ns. These have been found to propagate well in building power conductors in a differential mode, as demonstrated by Månsson (Månsson, September 2006).

For longer waveforms, it appears that pulse widths on the order of 100 μ s can create damage to equipment power supplies and to circuit boards at levels as low as 500 volts, but more typically at levels of 2–4 kV (IEC61000-2-5, 2010). The electric

fast transient (EFT) pulse (5/50 ns) used in EMC testing will produce serious equipment malfunction and damage at levels of 4–5 kV/m.

Hence, it is necessary to improve the SE of the building since most of the electrical and electronic devices are placed within a building. It is possible to reside all the sensitive electrical devices into the shielding room but it is very expensive to build.

2.3 Theory of Shielding Effectiveness

In the electrical and electronic circuit design, shielding is a common technique applied by circuit designers with the aim of reducing excessive emission from the PCB and providing sufficient immunity to the EM wave (Montrose, 1998; Saizalmursidi & Zarar, 2011). The term ‘shield’ usually refers to a metallic enclosure that completely encloses an electronic product. Shielding has no effect on a system but, when containing emissions, provides good immunity and does not require alteration of the board layout. There are two main purposes for shielding: preventing the coupling of undesired radiated electromagnetic energy into electrical devices inside the shield and preventing emissions of the product from radiating outside the boundaries of the electronics of the product, as illustrated in Figure 2.1.

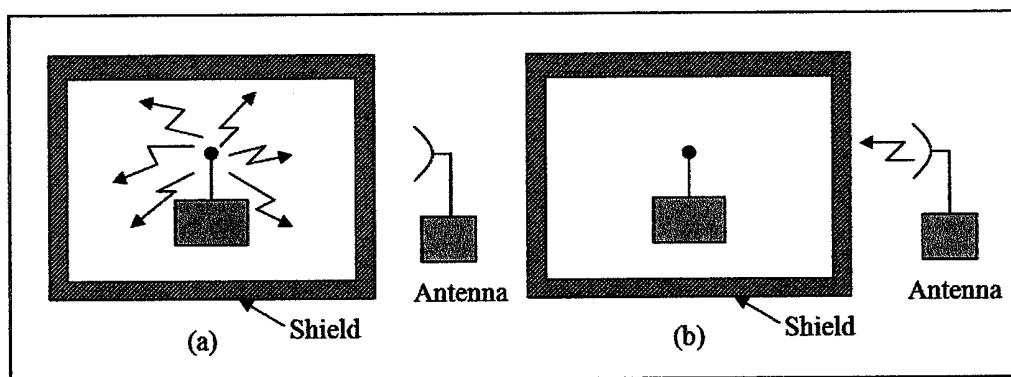


Figure 2.1: Illustration of a use of shielded enclosure. (a) To contain radiated emissions. (b) To exclude radiated emissions (Paul, 2006).

This concept had been applied on the screened room or shielding room and reverberation chamber, where a high level of isolation between the external environment and the internal space within the enclosure can be achieved (Leferink, 2010; Marvin et al., 2004). This room is built so that EMC test can be conducted and the result will not be influenced by the surrounding ambient EM wave.

Conceptually, a shield is a barrier to the transmission of EM fields. The effectiveness of a shield is considered as the ratio of the magnitude of electric field that is incident on the barrier to the magnitude of the electric field that is transmitted through the barrier.

The figure-of-merit used to determine the effectiveness of a metallic enclosure is SE. It can be defined at each of the point in the enclosure. In an effort to realise an ideal value of SE, the shield must completely enclose the electronics and must have no penetrations, such as holes, seams, slots or cable. Any penetration in a shield could drastically reduce the effectiveness of the shield. Effectively treating all penetrations provides the effective use of shields for electronics products.

There are two ways of approaching the theory of shielding which are based on the circuit theory and field theory. The field theory approach is based on the field propagation in free space to yield the value of SE (Paul, 2006), whereas the circuit theory approach employs the transmission line theory to predict the field strength at any given distance from the shielding barrier material (Brush, Schulz, & Plantz, 1988).

In order to express the general idea of SE, the general problem of a metallic barrier of thickness t , conductivity σ , relative permittivity ϵ_r and relative permeability μ_r , as shown in Figure 2.2.

An EM wave is incident on the barrier. A part of the incident EM wave is reflected and the remaining part of the EM wave is transmitted through the barrier. The SE of the barrier is defined in decibels as eq. (2.1). P_i represents the power density at a measuring point before the shield and P_t represents the power density at the same measuring point after the shield.

$$SE_{dB} = 10 \log_{10} \left(\frac{P_i}{P_t} \right) \quad (2.1)$$

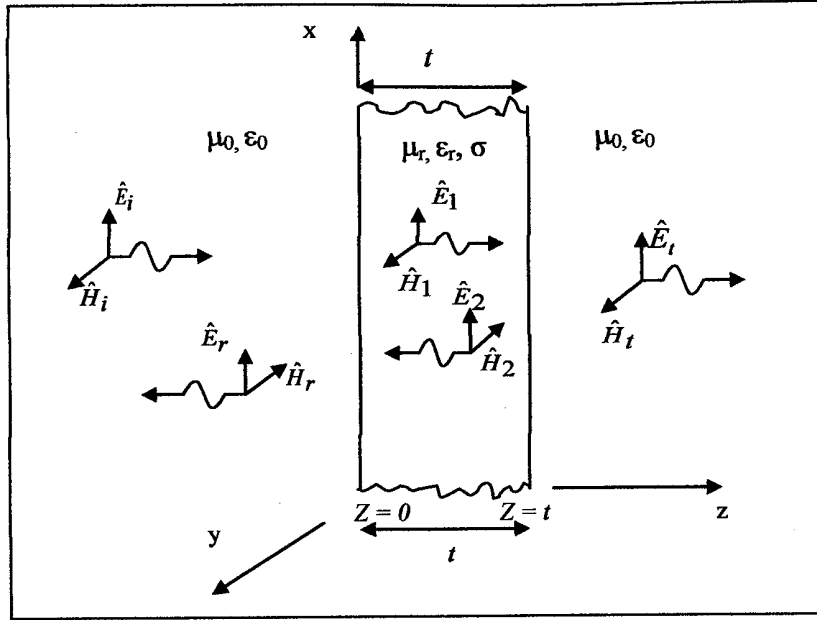


Figure 2.2: Representation of shielding phenomenon for plane waves (Paul, 2006).

It should be noted that eq. (2.1) is always positive, since the incident power density is expected to be greater than the transmitted power density. The power density in W/m^2 also can be expressed as the product of electric field, E (V/m) multiplied by magnetic field, H (A/m). Therefore, SE can also be written as eq. (2.2). \hat{E}_i and \hat{H}_i represent the intensity of incident electric and magnetic field respectively. On the other hand, \hat{E}_t and \hat{H}_t represents the intensity of transmitted electric and magnetic field respectively.

$$SE_{dB} = 10 \log_{10} \left(\frac{\hat{E}_i \hat{H}_i}{\hat{E}_t \hat{H}_t} \right) \quad (2.2)$$

If the relationship between the electric and magnetic field is represented by wave impedance in eq. (2.3), eq. (2.2) will become eq. (2.4) or eq. (2.5).

$$\hat{Z}_w = \frac{\hat{E}}{\hat{H}} \quad (2.3)$$

$$SE_{dB} = 20 \log_{10} \left(\left| \frac{\hat{E}_i}{\hat{E}_t} \right| \right) \quad (2.4)$$

$$SE_{dB} = 20 \log_{10} \left(\left| \frac{\hat{H}_i}{\hat{H}_t} \right| \right) \quad (2.5)$$

Equations eq. (2.4) and eq. (2.5) provide identical results only in the far field conditions but do not result in the same SE in the near field since the wave impedances relationship are not equivalent. The definition of the SE in eq. (2.4) is usually taken to be standard for either situation.

There are several phenomena contributing to the reduction of the incident field as it passes through the barrier, namely reflection loss (R_{dB}), absorption loss (A_{dB}) and multiple reflection loss (M_{dB}). The diagram shown in Figure 2.3 illustrates the conceptual mechanism of SE. The first mechanism is a reflection at the first surface of the barrier. When the incident field impinges on the surface of the barrier, a part of the incident electric field is reflected based on the reflection coefficient for that surface and the remaining part of the field will penetrate into the barrier.

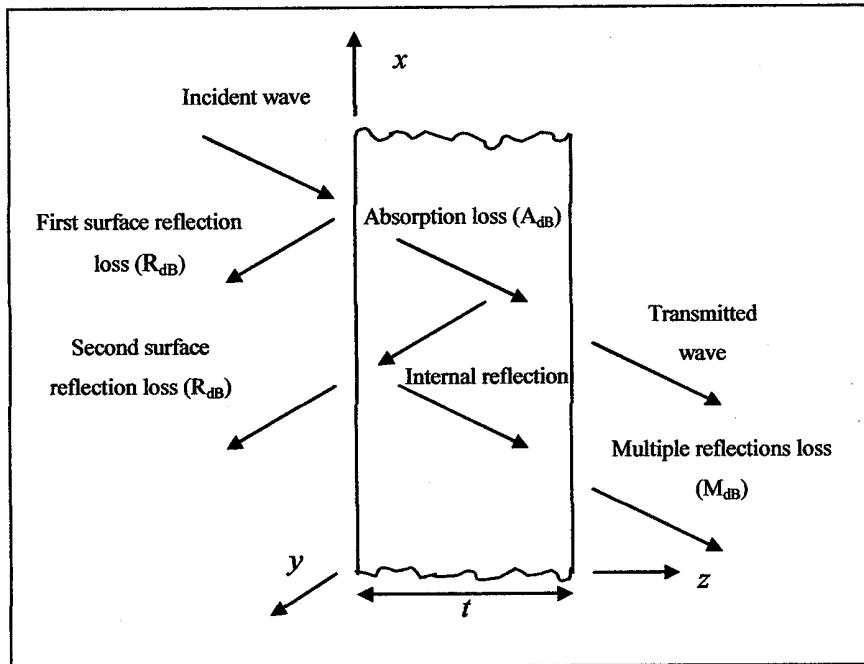


Figure 2.3: Illustration of losses within a shield.

The amplitude of incident field is attenuated as it passes through the barrier according to the factor $e^{-\alpha z}$ as shown in Figure 2.4, where α is the attenuation constant of the material, z is the distance of propagation. The reduction of the field is referred to as absorption loss. The attenuation constant, α for barrier materials that comprise a good conductor is related to the skin depth of the material, δ as $\alpha = 1/\delta$. Therefore, the amplitudes of the fields are attenuated according to the factor $e^{-z/\delta}$. If the barrier thickness t is much greater than the skin depth, δ of the barrier material at the frequency of the incident wave, the transmitted wave in the first boundary is greatly attenuated when it strikes the second boundary. The reflected part of this wave is transmitted back through the barrier and strikes the first boundary. This becomes the incident wave for the second boundary. A part of this incident wave is reflected, and the remaining part is transmitted across the barrier into the medium on the second boundary of the barrier. Between the two surfaces, there will be multiple reflections that may be overlooked if the absorption loss in the barrier is at least 15 dB (Brush et al., 1988).

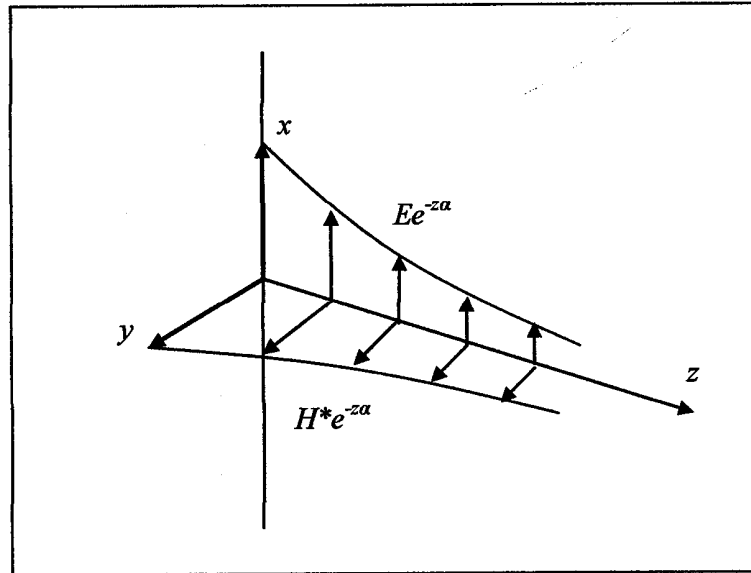


Figure 2.4: The absorption loss in a screen decreases exponentially and is reduced by $1/e$ at a distance z equal to the penetration.

The SE may be defined as the sum of three terms, which are reflection loss, absorption loss, and multiple reflections, as in eq. (2.6).

$$SE_{dB} = A_{dB} + R_{dB} + M_{dB} \quad (2.6)$$

where R_{dB} represents the reflection loss in decibel caused by reflection at the left and right interfaces, These parameters can be calculated based on eq. (2.7) – eq. (2.12) (Paul, 2006). A_{dB} represents the absorption loss in decibel as the wave proceeds through the barrier, M_{dB} represents the additional effects of multiple reflections and transmission, η_o is the intrinsic impedance of free space, 120π , η is the characteristic impedance of the material, μ_r is the relative permeability of the material, μ_o is the permeability of free space ($1.2566 \times 10^{-6} \text{ mkg s}^{-2} \text{ A}^{-2}$), ϵ_r is the dielectric constant (real part of relative permittivity) of the material. f is the operating frequency, γ is the propagation constant of the material, t is the thickness of the material. ϵ_o is the permittivity of free space ($8.854 \times 10^{-12} \text{ m}^{-3} \text{ kg}^{-1} \text{ s}^4 \text{ A}^2$), LT is the loss tangent of the material, ϵ_i is the loss factor (imaginary part of relative permittivity of the material).

$$R_{dB} = 20 \log \left| \frac{(\eta_o + \eta)^2}{4\eta_o \eta} \right| \quad (2.7)$$

$$A_{dB} = 20 \log |e^{\gamma t}| \quad (2.8)$$

$$M_{dB} = 20 \log \left| 1 - \left(\frac{\eta_o - \eta}{\eta_o + \eta} \right)^2 e^{-2\gamma t} \right| \quad (2.9)$$

$$\eta = \sqrt{\frac{j\mu_r\mu_o}{\epsilon_o\epsilon_r(LT + j)}} \quad (2.10)$$

$$\gamma = \sqrt{j\omega^2\mu_o\mu_r\epsilon_o\epsilon_r(LT + j)} \quad (2.11)$$

$$LT = \frac{\epsilon_i}{\epsilon_r} \quad (2.12)$$

2.3.1 Near-field and Far-field Shielding

The characteristic of the incoming EM field are dependent on the source (antenna), the medium surrounding the source, and the distance between the source and the point of observation. The space surrounding the source is divided into two regions, as shown in Figure 2.5. At a distance greater than $\lambda/2\pi$, it is the far or radiation field. In this region, the plane-wave conditions assume that the field is fully developed, and the ratio of the electric field (E-field) and magnetic field (H-field) is equal to the wave impedance of the free space ($\hat{E}_i / \hat{H}_i = \eta_o = 377\Omega$). The amplitude of the E-field and H-field are inversely proportional to the distance of observation ($1/r$). However, at a distance of less than $\lambda/2\pi$, the relationship between the E-field and H-field is complex and determined by the characteristics of the source and the distance from the source to the observation point. This is known as the near or induction field.

If the source has a high current and low voltage ($\hat{E}_i / \hat{H}_i < 377\Omega$), such as those produced by the loop antenna, the near field is predominantly magnetic. Conversely, if the source has low current and high voltage ($\hat{E}_i / \hat{H}_i > 377\Omega$), the near field is predominantly electric (Ott, 2009).

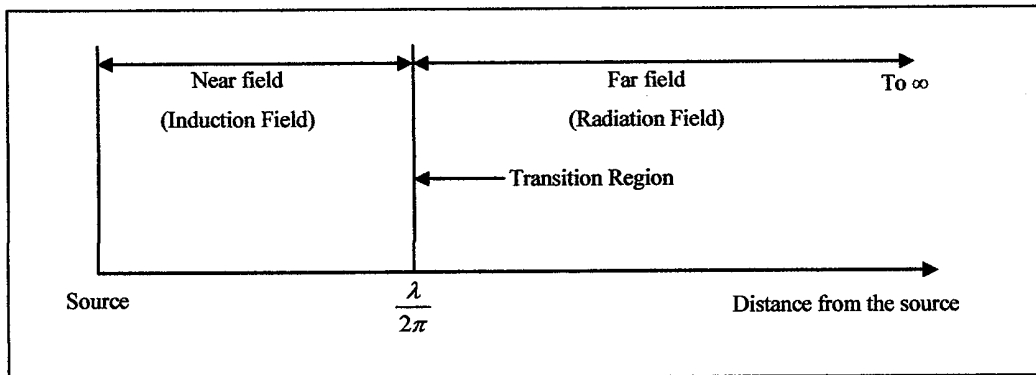


Figure 2.5: The space surrounding a source of radiation is divided into near field and far field. The transition from the near field to far field occurs at distance $\lambda/2\pi$.

The technique for shielding in the near-field is dependent on the type of source, either magnetic field source or electric field source. The analysis of the SE in the near field region is far more complicated if compared to far-field analysis, and the results are obtained based on the approximations to the exact results (P. Bannister, 1969; P. R. Bannister, 1968; Olsen, Istenic, & Zunko, 2003). Through this approximation, the intrinsic impedance of the free space is replaced with the wave impedance of the Hertzian (electric) dipole or small magnetic loop (dipole) (Olsen et al., 2003) dependent on the source of radiation.

The wave impedance for an electric dipole source is eq. (2.13). It is reduced to eq. (2.15) in the near field where r is the distance from the source, β_o is the propagation constant in free space, and λ_o is the wavelength in free space.

$$Z_{we} = \eta_o \frac{\frac{j}{\beta_o r} + \frac{1}{(\beta_o r)^2} - \frac{j}{(\beta_o r)^3}}{\frac{j}{\beta_o r} + \frac{1}{(\beta_o r)^2}} \quad (2.13)$$

$$Z_w \cong \eta_o \frac{-j}{\beta_o r} = \frac{\eta_o}{\beta_o r} \angle -90^\circ \quad (2.14)$$

Near field, $\beta_o r \ll 1$

$$|Z_{we}| = \frac{60\lambda_o}{r} \quad (2.15)$$

On the other hand, however, if the source is a magnetic dipole (loop), its wave impedance is eq. (2.18).

$$Z_{wm} = -\eta_o \frac{\frac{j}{\beta_o r} + \frac{1}{(\beta_o r)^2} - \frac{j}{(\beta_o r)^3}}{\frac{j}{\beta_o r} + \frac{1}{(\beta_o r)^2}} \quad (2.16)$$

$$Z_w \cong -j\eta_o\beta_or \angle -90^\circ \quad (2.17)$$

Near field, $\beta_or \ll 1$

$$|Z_{wm}| = \frac{2369r}{\lambda_o} \quad (2.18)$$

As an approximation, in order to apply eq. (2.6) for the near-field source, the intrinsic impedance of the free space η_o is replaced with the wave impedance (Z_{we} or Z_{wm}) of the source.

2.4 SE Determination

The SE determination can be carried out based on experiment measurements and analytical calculations, as shown in Figure 2.6. The details related to the process of obtaining the SE is described in the following paragraphs.

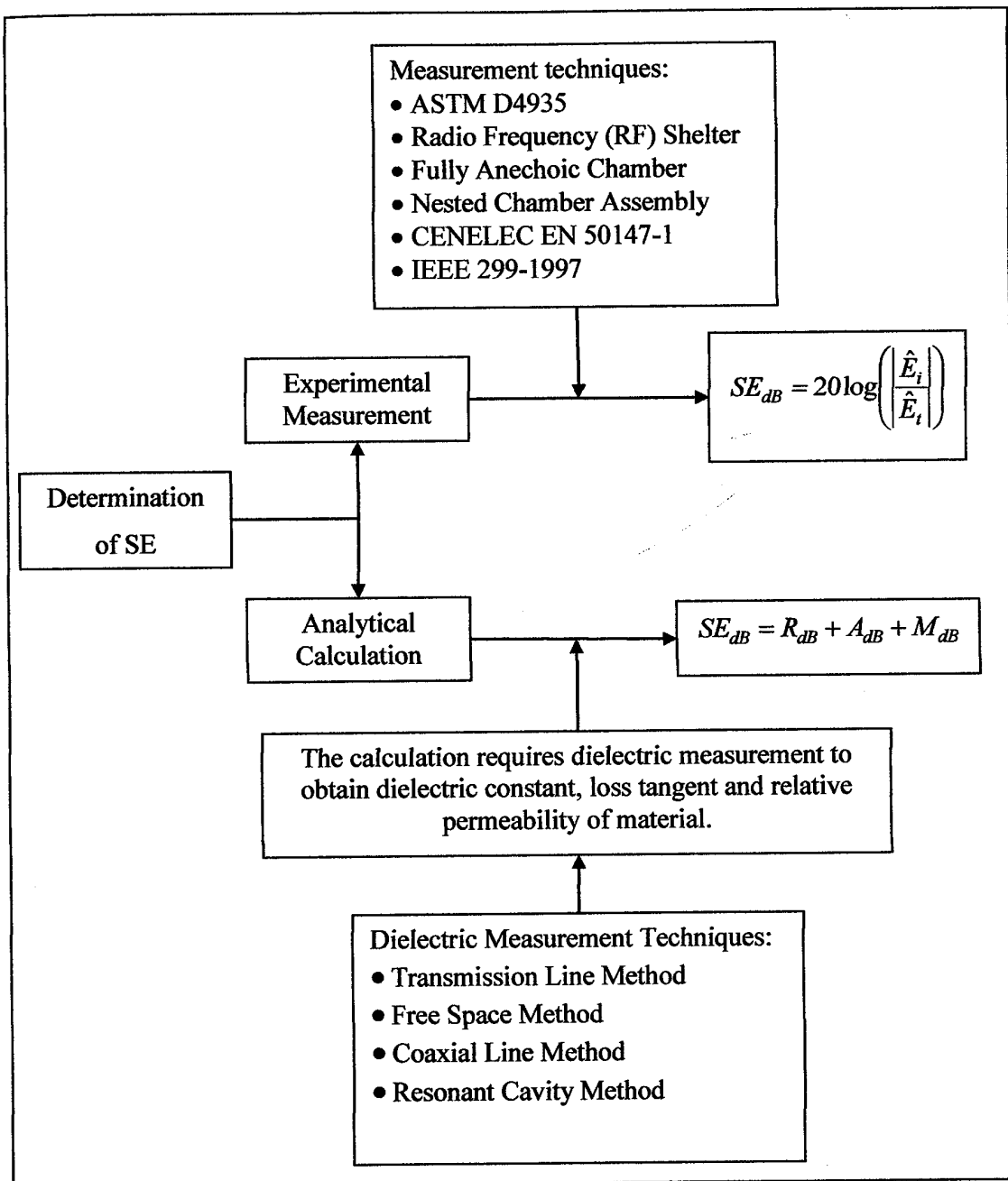


Figure 2.6: SE determination

Since the building materials are usually heavy, material testing on a small scale is preferred in the preliminary stage, such as through the test method which is based on standard ASTM D4935 (ASTM-D4935-10). This fixture is designed to be an enlarged section of a coaxial transmission line, which may be separated so as to allow for the inclusion and testing of planar materials. The test fixture is connected to a network analyser (NA), whilst a sample that is usually a thin solid layer is secured between the two coaxial halves. The NA is then used to measure the insertion loss, or S_{21} of the reference and load samples. The ratio of the S_{21} values provides a measure of the material SE. Thus, a small sample test can provide a rough estimate of the effect that different components may have on the shielding capabilities of the sample. It helps to reduce the expense and labour needed to construct and evaluate large concrete samples.

In order to obtain a more accurate representation of the attenuation effects of the building material, large sample test is also executed (Fan, Panitz, Greedy, Ngu, & Christopoulos, 2010; Frenzel, Stumpf, & Koch, 2007; Krause, 2012; Pruksanubal, 2011; Savage, Gilbert, Radasky, & Madrid, 2010). The larger scale test is based on the radio frequency (RF) shelter (Krause, 2012), fully anechoic chamber with specially designed enclosure to mount the building material (Frenzel et al., 2007; Pruksanubal, 2011) based on CENELEC EN 50147-1 and IEEE 299-1997, single antenna or receiver based on external ambient RF sources (Savage et al., 2010), and nested chamber assembly (reverberation chamber with smaller chamber) (Fan et al., 2010). Larger sample test is effort-consuming, and requires detailed setup to ensure the reliability of the result.

In the testing based on the RF shelter (Krause, 2012), a conductive concrete slab is poured into a 2 foot square plate of steel pre-cut with a 4 inch aperture on the centre to match the test port. In this work, 4-inch is proposed as it is more economical and manageable when considering the size of slabs and the existing wall structure of the shelter. Steel plates are used to ensure good electrical contact between the concrete slab and RF shelter. RF copper gaskets are placed between the two surfaces to provide an RF seal between the steel plate and the shelter wall. When the conductive concrete slab is affixed to the RF shelter over the test port, sufficient clamping pressure is employed to ensure electrical continuity between the steel plate and the shelter. However, the 4 inch test port behaves as an aperture below cut-off frequency, reducing the dynamic range of the test configuration below 100 MHz

REFERENCES

- Antonini, G., Orlandi, A., & D'elia, S. (2003). Shielding effects of reinforced concrete structures to electromagnetic fields due to gsm and umts systems. *IEEE Transactions on Magnetics*, 39(3), 1582-1585.
- ASTM-D4935-10. Standard Test Method for Measuring the Electromagnetic Shielding Effectiveness of Planar Materials.
- Bäckström, M. (1999). HPM testing of a car: a representative example of the susceptibility of civil systems. *Proceedings of 13th International Zurich Symposium and Technical Exhibition on EMC*, 189-190.
- Baker-Jarvis, J. (1990). *Transmission/reflection and short-circuit line permittivity measurements*: National Institute of Standards and Technology Colorado.
- Balanis, C. A. (1969). Technical Note : Measuring Of Dielectric Constants and Loss Tangent at E-Band Using A Fabry-Perot Interferometer.
- Bannister, P. (1969). Further notes for predicting shielding effectiveness for the plane. *IEEE Transactions on Electromagnetic Compatibility*, EMC-11(2), 50-53.
- Bannister, P. R. (1968). New theoretical expressions for predicting shielding effectiveness for the plane shield case. *IEEE Transactions on Electromagnetic Compatibility*, EMC-10(1), 2-7.
- Bantsis, G., Mavridou, S., Sikalidis, C., Betsiou, M., Oikonomou, N., & Yioultsis, T. (2012). Comparison of low cost shielding-absorbing cement paste building materials in X-band frequency range using a variety of wastes. *Ceramics International*, 38(5), 3683-3692.
- Bantsis, G., Sikalidis, C., Betsiou, M., Yioultsis, T., & Xenos, T. (2011). Electromagnetic absorption, reflection and interference shielding in X-band frequency range of low cost ceramic building bricks and sandwich type ceramic tiles using mill scale waste as an admixture. *Ceramics International*, 37(8), 3535-3545.